Dendrite-Free Electrodeposition and Reoxidation of Lithium-Sodium Alloy for Metal-Anode Battery

*Johanna K. Star[1], Yi Ding[2], and Paul A. Kohl[1,]**

1. School of Chemical and Biomolecular Engineering

Georgia Institute of Technology,

Atlanta, Georgia 30332-0100, USA

2. US Army RDECOM-TARDEC

AMSRD-TAR-R, MS 159

6501 E. 11th Street

Warran, MI 48397-5000

* Corresponding author. Email: kohl@gatech.edu

UNCLASSIFIED: Distribution Statement A. Approved for public release.

Report Documentation Page

Form Approved
OMB No. 0704-0188

1. REPORT DATE	2. REPORT TYPE	3. DATES COVERED
01 NOV 2011	**Journal Article**	**01-11-2011 to 01-11-2011**

4. TITLE AND SUBTITLE
DENDRITE-FREE ELECTRODEPOSITION AND REOXIDATION OF LITHIUM-SODIUM ALLOY FOR METAL-ANODE BATTERY

5a. CONTRACT NUMBER
US001-0000245070

5b. GRANT NUMBER

5c. PROGRAM ELEMENT NUMBER

6. AUTHOR(S)
Yi Ding; Paul Kohl; Johanna Star

5d. PROJECT NUMBER

5e. TASK NUMBER

5f. WORK UNIT NUMBER

7. PERFORMING ORGANIZATION NAME(S) AND ADDRESS(ES)
School of Chemical and Biomolecular Engineering,Georgia Institute of Technology,Atlanta,GA,30332-0100

8. PERFORMING ORGANIZATION REPORT NUMBER
; #22212

9. SPONSORING/MONITORING AGENCY NAME(S) AND ADDRESS(ES)
U.S. Army TARDEC, 6501 E.11 Mile Rd, Warren, MI, 48397-5000

10. SPONSOR/MONITOR'S ACRONYM(S)
TARDEC

11. SPONSOR/MONITOR'S REPORT NUMBER(S)
#22212

12. DISTRIBUTION/AVAILABILITY STATEMENT
Approved for public release; distribution unlimited

13. SUPPLEMENTARY NOTES

14. ABSTRACT
Two ionic liquids, EMI-AlCl4 and N1114-TFSI, that support both lithium and sodium deposition/dissolution were studied as potential electrolytes for lithium metal batteries. In both cases lithium?s dendritic growth was suppressed by adding a small amount of sodium to a lithium electrolyte. This results in a co-deposition or alloying process that hinders dendrite growth. SEM images show a significant difference in morphology obtained by the addition of sodium. A smooth deposit was not enough for stable cycling of the lithium anode because of lithium?s reactivity with the electrolyte. Vinylene carbonate (VC) was added to the N1114-TFSI to form a stable SEI layer. Cyclic voltammetry and chronopotentiometry was carried out on tungsten and stainless steel electrodes to obtain efficiency measurements. The combination of a small amount of sodium in the electrolyte, along with VC as an SEI former, lead to significant improvements in cycling performance and efficiency.

15. SUBJECT TERMS

16. SECURITY CLASSIFICATION OF:			17. LIMITATION OF ABSTRACT	18. NUMBER OF PAGES	19a. NAME OF RESPONSIBLE PERSON
a. REPORT	b. ABSTRACT	c. THIS PAGE			
unclassified	**unclassified**	**unclassified**	**Same as Report (SAR)**	**22**	

Abstact

Two ionic liquids, EMI-$AlCl_4$ and N_{1114}-TFSI, that support both lithium and sodium deposition/dissolution were studied as potential electrolytes for lithium metal batteries. In both cases, lithium's dendritic growth was suppressed by adding a small amount of sodium to a lithium electrolyte. This results in a co-deposition or alloying process that hinders dendrite growth. SEM images show a significant difference in morphology obtained by the addition of sodium. A smooth deposit was not enough for stable cycling of the lithium anode because of lithium's reactivity with the electrolyte. Vinylene carbonate (VC) was added to the N_{1114}-TFSI to form a stable SEI layer. Cyclic voltammetry and chronopotentiometry was carried out on tungsten and stainless steel electrodes to obtain efficiency measurements. The combination of a small amount of sodium in the electrolyte, along with VC as an SEI former, lead to significant improvements in cycling performance and efficiency.

Introduction

The deposition and re-oxidation of lithium metal is of interest for its potential use as the anode in lithium metal batteries. The lithium-metal anode has the highest possible theoretical capacity since only a current collector is needed to support the deposition of the metal. The density of lithium metal is 534 kg/m^3 giving it a capacity of 7369 coulombs/cm^3 (A s/cm^3) or 13,903 coulombs/g (A s/g) (*1*). The use of lithium metal reduction/oxidation as the anode half reaction would eliminate the need for an anode structure, such as carbon or silicon, thus lowering cost, size and weight of the battery as well as the assembly complexity.

However, the dendritic growth of lithium during cycling lowers the coulombic efficiency because the dendrite can become isolated from the anode if the base of the dendrite is oxidized before the tip. Lithium dendrites are a severe safety concern because dendrites can short circuit the anode and cathode. Anode-cathode short circuits are especially dangerous when a flammable organic solvent is used as the electrolyte.

Dendritic growth has been studied and various mechanisms have been proposed (*2-5*), however, only modest progress has been made in their elimination. Previous reports have shown that the lithium-anode cycle life can be extended by assembling a pressurized coin cell; however, this does not eliminate dendrite growth or address the fundamentals of their formation (*6*). Restricting the anode volume and applying pressure forces denser deposit, but the system still possesses the driving force for dendritic growth. Hydrofluoric acid has also been shown to suppress dendrites but it introduces an additional safety concern (*7*).

In this work, we studied the effect of alloying lithium metal with a small amount of sodium in order to suppress dendritic growth. It is thought that alloying lithium with another alkali metal would alter the rate or mechanism of dendrite growth, analogous to other dendritic metals such as tin and silver. The use of ionic liquids as the electrolyte for deposition mitigates flammability concerns associated with organic electrolytes. Ionic liquids have a wide electrochemical working range which makes them valuable in the deposition of lithium and sodium (*8-10*). The more negative redox potential of lithium and sodium metal compared to a carbon anode makes the stability of the ionic liquid very important. In fact, sodium is especially difficult to deposit electrochemically and ionic liquids are one of the only electrolytes usable (*8, 11*). Lithium deposition experiments have been carried out in ionic liquid electrolytes (*10-13*), however, the electrochemical deposition of lithium-sodium alloys has not been reported.

Although the non-dendritic growth of lithium addresses some of the safety issues, the electrochemical instability of lithium in contact with the electrolyte causes self-discharge and capacity loss through reaction of the metal with the electrolyte. It has been reported that the formation of a stable, solid electrolyte interface (SEI) is necessary for graphite-based anodes to achieve stable performance and low self-discharge. The SEI layer is formed using the electrolyte itself or an additive in the electrolyte (*12-14*). SEI formation by itself, as previously reported (*15-16*), is not an effective strategy for full dendrite elimination or high coulombic efficiency because of the high surface area and volume changes of the deposit. If the SEI layer were formed over a dendrite, it would leave a high surface area, empty shell upon reoxidation of the metal. In this study, an efficient SEI layer is formed on the non-dendritic lithium-sodium alloy so as to minimize its reformation upon cycling.

Experimental

Ethyl-methyl-imidazolium chloride (EMI^+Cl^-, 97%, Acros) and aluminum chloride (anhydrous, Fluka) was used as-received. Ethyl-methyl-imidazolium chloroaluminate (EMI-$AlCl_4$) was synthesized by buffering an acidic melt of EMI^+Cl^- and $AlCl_3$ with either lithium chloride (99%, Baker) or sodium chloride depending on the desired electrolyte.

$$EMI^+Cl^- + AlCl_{3\,(excess)} \rightarrow EMI^+ + AlCl_4^- \quad [1]$$

$$AlCl_4^- + AlCl_3 \rightarrow Al_2Cl_7^- \quad [2]$$

$$Al_2Cl_7^- + MCl \rightarrow M^+ + 2AlCl_4^- \quad [3]$$

The initial melt was made by slowly mixing the EMI^+Cl^- and $AlCl_3$ in a 55:45 molar ratio until only a clear liquid remained (Equations 1, 2). This liquid was dried under vacuum for 8 h before adding 100% excess of the metal chloride to ensure a completely buffered melt (Equation 3). In order for this melt to give reversible plating/dissolution, ~0.005 wt% of $SOCl_2$ was added to each melt (*17-19*). Ionic liquids containing both sodium and lithium salts were mixed by volume from separate single salt melts. The working electrode was a 0.5 mm diameter tungsten wire and the counter electrode was a 1 mm diameter tungsten wire. Both were encased in borosilicate glass and polished before each use.

Trimethylbutylammonium bis(triflouromethanesulfonyl)imide (N_{1114}-TFSI, 99%, Iolitec) and lithium bis(triflouromethanesulfonyl)imide (LiTFSI, 99%, Acros) were used as-received. Sodium bis(triflouromethanesulfonyl)imide (NaTFSI) was synthesized by the reaction of

triflouromethanesulfonylimide (HTFSI, Wako) with a 1M NaOH solution until the solution was pH neutral. The solution was heated to 60°C and dried under vacuum for 10 h to remove water. N_{1114}-TFSI ionic liquids were made by dissolving the appropriate amount of metal TFSI salt followed by drying for several hours before each use. The working and counter electrodes used with this ionic liquid were type 305 stainless steel foils.

All work was performed in an argon filled Vacuum Atmospheres glovebox. Electrochemical experiments were carried out with a Perkin Elmer Parstat Model 2263 poteniostat/galvanostat interfaced with a computer running PowerSuite software. The reference electrode for all experiments was an aluminum wire (Fluka) immersed in a 40:60 mol ratio EMI^+Cl^-:$AlCl_3$ melt in a fritted glass tube. The electrochemical couple is between the acidic chloroaluminate species and the metallic aluminum, as described by Equation 4.

$$4Al_2Cl_7^- + 3e^- \rightarrow Al + 7AlCl_4^- \qquad E=0.0\ V\ (-0.03\ V\ vs.\ NHE\ (\textit{20})) \qquad [4]$$

Electrochemical measurements were carried out in a beaker cell with electrodes spaced less than 1 cm apart.

Scanning electron microscopy (SEM) was used to study the morphology of different deposits. For the SEM sample, metal was deposited on the appropriate foil. Images were taken with a Zeiss Ultra 60 SEM.

Results and Discussion

The initial ionic liquid selection was driven by the need to electrodeposit sodium and lithium from the same electrolyte at high coulombic efficiency. EMI-$AlCl_4$ has already been shown as a suitable electrolyte for the deposition of both metals (*17-18*) . More recent studies have focused on TFSI-based ionic liquids where it was shown that these too are suitable for depositing both lithium and sodium (*8, 21*).

Cyclic voltammograms (CV) on tungsten, Figure 1, demonstrate electrochemical reduction of the alkali metal cation to the alkali metal at potentials negative of -2.1 V and subsequent re-oxidation of the metal on the positive-going potential sweep. It is interesting to note that the reduction potential for Li^+ and Na^+ in EMI-$AlCl_4$ are each more positive than their standard potentials. Li^+ reduction starts -2.15 V and Na^+ at -2.45 V vs. Al/Al(III), compared to their standard potentials of -3.01 V and -2.68 V (-3.04 V and -2.71 V vs. NHE) for lithium and sodium, respectively (*22*). The separation of the reduction potentials between lithium and sodium in EMI-$AlCl_4$ is most likely due to an interaction with the chloroaluminate

anion, as no such shift occurs in imidazolium-based TFSI ionic liquids (*23*). In EMI-$AlCl_4$, lithium is reduced at a more positive potential than sodium, which makes deposition of an alloy more difficult.

The coulombic efficiency for deposition and reoxidation of the metal can be calculated from the voltammogram. The area of the reduction peak can be compared to the area of the oxidation peak, which is observed due to the exhaustion of oxidizable material where the current drops sharply to zero. This coulombic efficiency from Fig. 1 was 90% for lithium and 82% for sodium. For lithium, the loss of efficiency is likely due to the reaction of the electrolyte with the metal and the inefficiency of reoxidizing dendrites, as described above. Sodium also reacts with the electrolyte and the loss of efficiency here may be greater than that of lithium since its reduction occurs at more negative potentials.

An unbuffered acidic EMI-$AlCl_4$ electrolyte can reduced at -2.2 V on a tungsten electrode. The addition of $SOCl_2$ to the ionic liquid increases the stable potential range to -2.4 V, which coincides with the sodium reduction potential. There is a 200 mV overpotential and hysteresis for the reduction and reoxidation of sodium ions when deposited on a tungsten surface. The hysteresis and overpotential on the initial CV scan on tungsten has been attributed to the difficulty in nucleating sodium metal on a foreign surface (i.e. tungsten) possibly confounded by the presence of chloride or chloroaluminate species. Sodium oxidation also shows a low exchange current upon oxidation compared to lithium. The oxidation of sodium begins at a potential negative of lithium, however, the mass-limited oxidation peak does not occur until potentials positive of lithium.

Since ionic liquid electrolytes capable of producing both sodium and lithium metal are available, the focus of this study then shifts to the possible co-deposition of LiNa alloys and their potential suppress dendrite growth. A 1:1 volume combination of Li buffered EMI-$AlCl_4$ and Na buffered EMI-$AlCl_4$ ionic liquids was mixed and its behavior studied using cyclic voltammetry. Figure 2 shows the CVs for the 1:1 lithium:sodium mixture when scanned to several switching potentials. When the switching potential was -2.3 V, only a single oxidation peak was observed. This CV has many features in common with the CV from the pure lithium ionic liquid, Fig. 1. The reduction current is similar with onset potential of -2.15 V followed by a sharply defined, single oxidation peak. As the switching potential was made more negative (i.e. -2.5 V and -2.7 V), a second oxidation peak appears at -1.7 V upon scan reversal. This second peak matches closely to that seen for the pure sodium containing ionic liquid, Fig. 1, in potential and in slope. That is, the combined lithium:sodium ionic liquid appears to produce a deposit which is the linear sum of the two separate ionic liquids without extensive interaction or alloying of the two metals. While this may appear to be a surprise (lack of signs of alloying), it is noted that the shift in reduction potentials

does suggest a role for chloride or chloroaluminate intermediates on the surface which can disrupt the alloying effect.

To identify the composition of the two peaks in Fig. 2, inductively coupled plasma emission spectroscopy (ICP-ES) was carried out on the solid deposits formed at constant potential. Deposits were formed after the passage of 0.2 C of charge. It should be noted that removal of excess electrolyte on or in the deposits is a significant source of error in analysis. The ionic liquid is viscous and washing with DMC was necessary to remove residual electrolyte. In addition, the deposits made at different potentials may contain both metal regardless of whether alloying occurred because of the overlap in potentials for the two metals. The ICP results are shown in Table 1.

Lithium was deposited from a lithium buffered EMI-$AlCl_4$ ionic liquid to establish a baseline. The lithium deposit was then dipped in a sodium buffered ionic liquid to simulate contact with the mixed electrolyte (sample #1). The sample was rinsed with DMC to remove as much electrolyte as possible. This process introduced a 10% error in the elemental analysis. The analysis showed only 90.8% lithium and 9.2% sodium. The second and third samples shown in Table 1 were deposited from a 50%Li/50%Na EMI-$AlCl_4$ ionic liquid at different potentials. At -2.2 V (sample #2), only the single oxidation peak, associated with lithium, was observed in the CV. The deposit was essentially all lithium, within experimental error of the control sample, #1. At -2.6 V (sample #3), the CV clearly shows two oxidation peaks with one each associated with lithium and sodium. The elemental analysis shows that at this potential, the deposit is 80% sodium. Thus, we conclude the oxidation peak at -1.7 V is sodium or a sodium rich alloy, while the oxidation peak at -2.0 V is mostly due to lithium.

To further understand this double peak, the deposit morphology was analyzed by examining metal topography at several different potentials. SEM images of these deposits from a 90%Li/10%Na EMI-$AlCl_4$ ionic liquid are shown in Figure 3. For comparison, SEM images of deposits from a lithium-only EMI-$AlCl_4$ ionic liquid are shown in Figure 4.

The low current deposits (e.g. 1 mA/cm^2) produced from the pure lithium and 90%Li/10%Na ionic liquids looked the same in structure. Curling dendrites formed moss-like structures on the substrate surface. At higher current density however, the deposit changed significantly. At 5 mA/cm^2 and 7 mA/cm^2, the lithium deposit formed straight, sharp needles (Figure 4). Deposits produced from the 90%Li/10%Na ionic liquid showed only small, stunted, dendritic needles at 5 mA/cm^2. At higher current, 7 mA/cm^2, elongated structures were visible, but no sharp, pointed dendrites could be found.

Based on the potentials recorded in the chronopotentiometry experiments, the disappearance of dendrites coincides with the appearance of the second oxidation peak in the CV, as shown in Figure 2.

ICP results indicate that the appearance of the second peak coincides with an increase in sodium in the deposit. Thus it is likely that the co-deposition of sodium with the lithium hinders dendritic growth.

The suppression of dendritic growth could increase the coulombic efficiency for the deposition and reoxidation of the metal. Figure 5 shows the coulombic efficiency as calculated from the CV experiments as a function of switching potential from the Li buffered, Na buffered, and 50%Li/50%Na buffered EMI-$AlCl_4$ ionic liquids.

The maximum coulombic efficiency obtained for Lithium deposition/dissolution was 90% for a switching potential of -2.2 V. Scanning to more negative potentials lowers the efficiency because the EMI^+ reduction occurs within this potential range and a fraction of the charge goes toward the reduction of the electrolyte. For sodium, the highest efficiency was 82% at a switching potential of -2.6 V. At -2.5 V, small current peaks were recorded, but the background current was not negligible causing the efficiency to drop. Again, going to more negative potentials lowered the efficiency because of electrolyte reduction.

Figure 5 also shows the coulombic efficiency for a 50%Li/50%Na ionic liquid. The maximum efficiency for this electrolyte was 87% achieved at -2.6V. This efficiency is, unfortunately, not higher than that of the lithium-only case because the lithium concentration was lower causing the relative amount of charge going to lithium reduction (compared to the electrolyte and sodium reduction) to be lower when the potential was at less extreme values. At more extreme values needed for sodium reduction, the reduction of the electrolyte competes more effectively.

Although dendritic growth was successfully suppressed in the EMI-$AlCl_4$ system, the change in morphology did not lead to an increase in efficiency or cycle life. Use of a cyclic carbonate SEI formers was attempted, however, they formed precipitates in this electrolyte. This makes the EMI-$AlCl_4$ ionic liquid unsuitable for efficient lithium alloy cycling, as would be required for application in a lithium-metal anode battery.

Trimethylbutylammoniun TFSI (N_{1114}-TFSI) based ionic liquids have been shown to have better tolerance for water and oxygen contamination than their chloroaluminate counterparts.The shift in sodium and lithium reduction potentials described above in chloroaluminate ionic liquids do not occur to the same extent. This results in a more negative reduction potential which would lead to a higher voltage battery. N_{1114}-TFSI has previously been shown to support reversible lithium and sodium redox couples (*8, 21*). Electrochemical experiments were performed at a type 304 stainless steel working electrode. Figure 6 shows the CV behavior of 1M Li N_{1114}-TFSI, 0.3M Na N_{1114}-TFSI, and 1M Li/0.1M Na

N_{1114}-TFSI. The low solubility of NaTFSI in N_{1114}-TFSI did not allow for testing at higher sodium concentrations.

Coulombic efficiency was calculated by integration of the reduction and oxidation processes from the CV scans. The coulombic efficiency was 55% for 1M Li N_{1114}-TFSI and 54% for 0.3M Na N_{1114}-TFSI. The reduction potentials for the two metal ions are -2.85 V for sodium and -2.75 V for lithium, which are more negative compared to EMI-$AlCl_4$, but close to the theoretical redox potentials. Alloying of the metals is likely to occur in this system because their reduction potentials are nearly the same.

Alloy deposition was studied using a mixed ionic liquid containing 1M Li/0.1M Na in N_{1114}-TFSI. The ionic liquid was vacuum dried prior to use. The efficiency from the CV experiments in Figure 6 was 57%, which is slightly higher than that of the 1M Li N_{1114}-TFSI electrolyte. Contrary to the chloroaluminate ionic liquid, this mixture displayed only a single oxidation peak, indicating that an alloying process rather discrete deposition of the two metals occurred.

Chronopotentiometry experiments consisting of deposition for 100 s at 0.1 mA/cm^2 followed by reoxidation at the same current density were performed. The oxidation current was maintained until the voltage reached -1.5 V at which point the experiment was terminated. The efficiency was calculated from these chronopotentiomery experiments and the results are shown in Figure 7. The efficiency of 1M Li N_{1114}-TFSI ionic liquid increased through the first 10 cycles until a value of 70% was reached. The efficiency remained relatively constant for more than 100 cycles. No significant change in efficiency was observed with the ionic liquid mixture of 1M Li/0.1M Na in 1M Li in N_{1114}-TFSI compared to the 1M Li ionic liquid.

Although the coulombic efficiency of the lithium and lithium/sodium ionic liquids was similar, the morphology of the deposits was quite different. Figure 8 shows deposit morphology from each ionic liquid. The lithium-only deposit shows long dendrites that are 1-2 µm diameter. The 1M Li/0.1M Na ionic liquid, however, shows a porous, uniform film of uniform thickness with no dendrites. This deposit is most likely an alloy of the two metals based on the single peak observed from the CV scan and the more uniform nature of the deposit.

Again, the non-dendritic deposit alone did not improve the efficiency enough to make the electrolyte feasible for battery applications. The continued loss of efficiency is because of sustained reaction between the metal deposits and the electrolytes, which be attributed to the lack of an adequate SEI layer. Vinylene carbonate (VC) was evaluated as an SEI forming additive. In these experiments, 5wt% VC was added to a 1M Li/0.1M Na QATFSI electrolyte. CV and chronopotentiometry experiments were carried out as described before. The coulombic efficiency was calculated from CV

experiments was 60% (Figure 6), which is higher than the 1M Li or 1M Li/0.1M Na ionic liquids without VC. The cycling performance also greatly improved. The coulombic efficiency calculated from chronopotentiometry reached 85% within 30 cycles and reached a steady value of 90% through 100 cycles (Figure 7). This improvement is credited to a lower reaction rate between the deposit and the electrolyte. The chronopotentiometric efficiency is higher than that recorded from CV experiments because the continuous cycling allows the anode substrate to build up an effective SEI layer. Vinylene carbonate can react with the deposit over multiple cycles to form a stable film that prevents further reaction.

Conclusion

Two ionic liquids, EMI-$AlCl_4$ and N_{1114}-TFSI, have been studied as electrolytes for lithium metal batteries. Both have a large stability window to support lithium deposition and dissolution, making them candidates for lithium battery applications.

The approach to mitigating dendrite growth that currently prevents lithium metal anodes from becoming commercially viable was to add a small amount of sodium to the ionic liquid. There are two possible mechanisms for that would prevent dendrite growth in such a mixture. First, it is feasible to co-deposit the two metals. Because of the size mismatch between sodium and lithium atoms, a small amount of sodium can disrupt lithium's dendritic growth. A second possibility is to form an alloy of the two metals. This alloy can be potentially non-dendritic, even with a small amount of sodium, resulting in a smooth deposit.

A second problem is that lithium reacts with the electrolyte, causing capacity loss and blocking the substrate. This problem was approached with SEI forming additives. These additives can react with the deposited metal to form a stable, protective film that prevents further reaction.

In this work, we have shown that both EMI-$AlCl_4$ and N_{1114}-TFSI support non-dendritic deposits by the addition of a small amount of sodium to a lithium-based ionic liquid. Additives were studied with N_{1114}-TFSI and it was shown that 5% VC added to a 1M Li/0.1M Na N_{1114}-TFSI ionic liquid could help build a stable SEI, resulting in a cycling efficiency of 90% over 100 cycles.

Acknowledgements:

The authors gratefully acknowledge the financial support of the US Army, contract US001-0000245070.

References

1. Zhang, W., *Journal of Power Sources* **196**, 13-24 (2011).
2. L. Gireaud, S. Grugeon, S. Laruelle, B. Yreiex, J. Tarascon, *Electrochemistry Communications* **8**, 1639-1649 (2006).
3. J. Yamaki, S. Tobishima, K. Hayashi, K. Saito, Y. Nemoto, M. Arakawa, *Journal of Power Sources* **74**, 219-227 (1998).
4. M. Dolle, L. Sannier, B. Beaudoin, M Trentin, J. Tarascon, *Electrochemical and Solid-State Letters* **5**, A286-A289 (2002).
5. P. Howlett, D. MacFarlane, A. Hollenkamp, *Journal of Power Sources* **114**, 277-284 (2003).
6. T. Hirai, I. Toshimatsu, J. Yamaki, *Journal of the Electrochemical Society* **141**, 611-614 (1994).
7. K. Kanamura, S. Shiraishi, Z. Takehara, *Journal of the Electrochemical Society* **141**, L108-L110 (1994).
8. R. Wibowo, L. Aldous, E. Rogers, S. Ward Jones, R. Compton, *J. Phys. Chem.* **114**, 3618-3626 (2010).
9. Ketack Kim, Christopher Lang, Paul Kohl, *Journal of the Electrochemical Society* **152**, E56-E60 (2005).
10. J. Vega, J. Zhou, P. Kohl, *Journal of the Electrochemical Society* **156**, A253-A259 (2009).
11. G. Gray, J. Winnick, P. Kohl, *Journal of the Electrochemical Society* **143**, 3820-3824 (1996).
12. H. Zheng, K. Jiang, T. Abe, Z. Ogumi, *Carbon* **44**, 203-210 (2006).
13. A. Balducci, M. Schmuck, W. Kern, B. Rupp, S. Passerini, M. Winter, *ECS Transactions* **11**, 109-114 (2008).
14. X. Wang, H. Lee, H. Li, X. Yang, X. Huang, *Electrochemistry Communications* **12**, 386-389 (2010).
15. T. Mogi, M. Inaba, S. Jeong, Y. Iriyama, T. Abe, Z. Ogumi, *Journal of the Electrochemical Society* **149**, A1578-A1583 (2002).
16. J. Sakamoto, F. Wudl, B. Dunn, *Solid State Ionics* **144**, 295-299 (2001).
17. C. Lang, K. Kim, P. Kohl, *Electrochimica Acta* **51**, 3884-3889 (2006).
18. C. Scordilis-Kelley, R. Carlin, *Journal of the Electrochemical Society* **140**, 1606-1611 (1993).
19. K. Kim, C. Lang, P. Kohl, *Journal of the Electrochemical Society* **152**, E9-E13 (2005).
20. C. Scordilis-Kelley, J. Fuller, R. Carlin, J. Wilkes, *Journal of the Electrochemical Society* **139**, 694-699 (1992).
21. R. Wibowo, S. Ward, R. Compton, *J. Chem. Eng. Data* **55**, 1374-1376 (2010).
22. *Handbook of Chemistry and Physics*. R. Weast, Ed., (CRC Press Inc., ed. 69, 1988).
23. M. Egashira, H. Todo, N. Yoshimoto, M. Morita, J. Yamaki, *Journal of Power Sources* **174**, 560-564 (2007).

Table 1: ICP-ES results showing elemental analysis of deposits from MEIC ionic liquids.

Sample	Li (ppm)	Na (ppm)	Li (mol%)	Na (mol%)
(1) 1M Li, contaminated	22.1	2.24	90.8	9.2
(2) 50%Li/50%Na dep at -2.2V	13.9	1.67	89.3	10.7
(3) 50%Li/50%Na dep at -2.6V	5.46	22	19.9	80.1

Figure Captions:

1. CV of Lithium and Sodium buffered MEIC melts at 100mV/s.
2. CV of a 1:1 mixture of Sodium and Lithium buffered MEIC melts at 100mV/s.
3. SEM images of deposits from a 90%Li/10%Na buffered MEIC melt. Metal was deposited at the current shown until a charge of 5 C/cm^2 was reached.
4. SEM images of typical deposits from a lithium buffered MEIC ionic liquid.
5. Coulombic efficiencies calculated from CV at different switching potentials.
6. CV of 1M Li, 0.3M Na, and 1M Li/0.1M Na in QATFSI. Coulombic efficiencies were 55% for Lithium, 50% for Sodium, and 57% for the mixture. The scan rate was 10mV/s.
7. Cycling experiments at 0.1 mA/cm2 for 100 s.
8. SEM images of deposit from a 1M Li electrolyte and a 1M Li/0.1M Na electrolyte. A constant current of 0.5mA/cm^2 was applied for 1000s for 0.5C/cm^2.

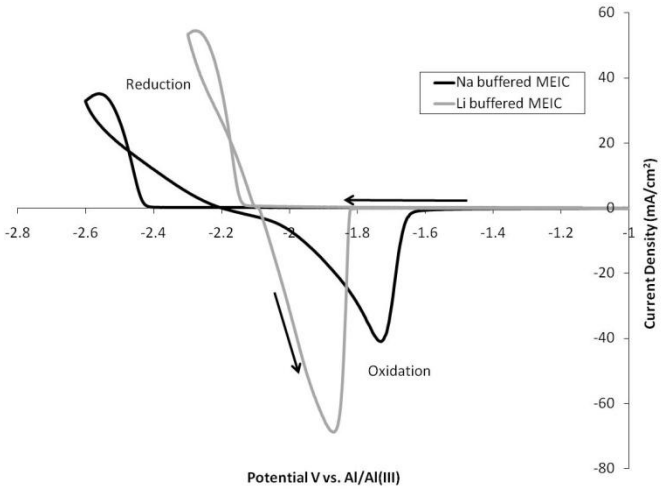
Reduction
Na buffered MEIC
Li buffered MEIC
Oxidation
Potential V vs. Al/Al(III)
Current Density (mA/cm²)
60
40
20
0
-20
-40
-60
-80
-2.8
-2.6
-2.4
-2.2
-2
-1.8
-1.6
-1.4
-1.2
-1

Figure 1

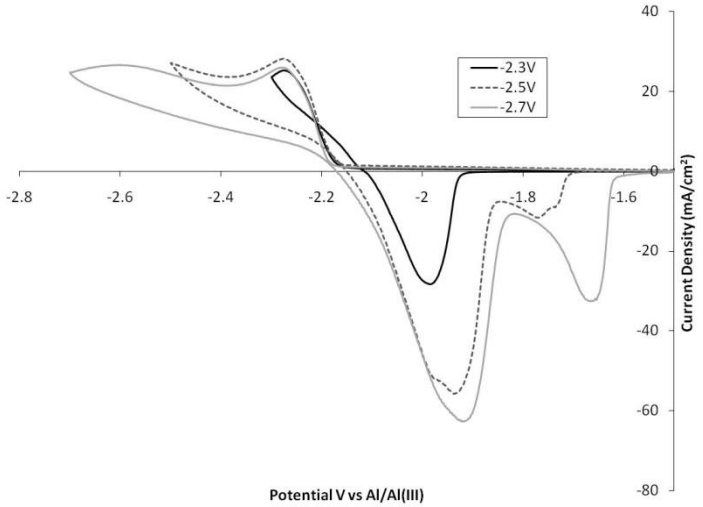
-2.3V
-2.5V
-2.7V
40
20
0
-20
-40
-60
-80
-2.8
-2.6
-2.4
-2.2
-2
-1.8
-1.6
Current Density (mA/cm²)
Potential V vs Al/Al(III)

Figure 2

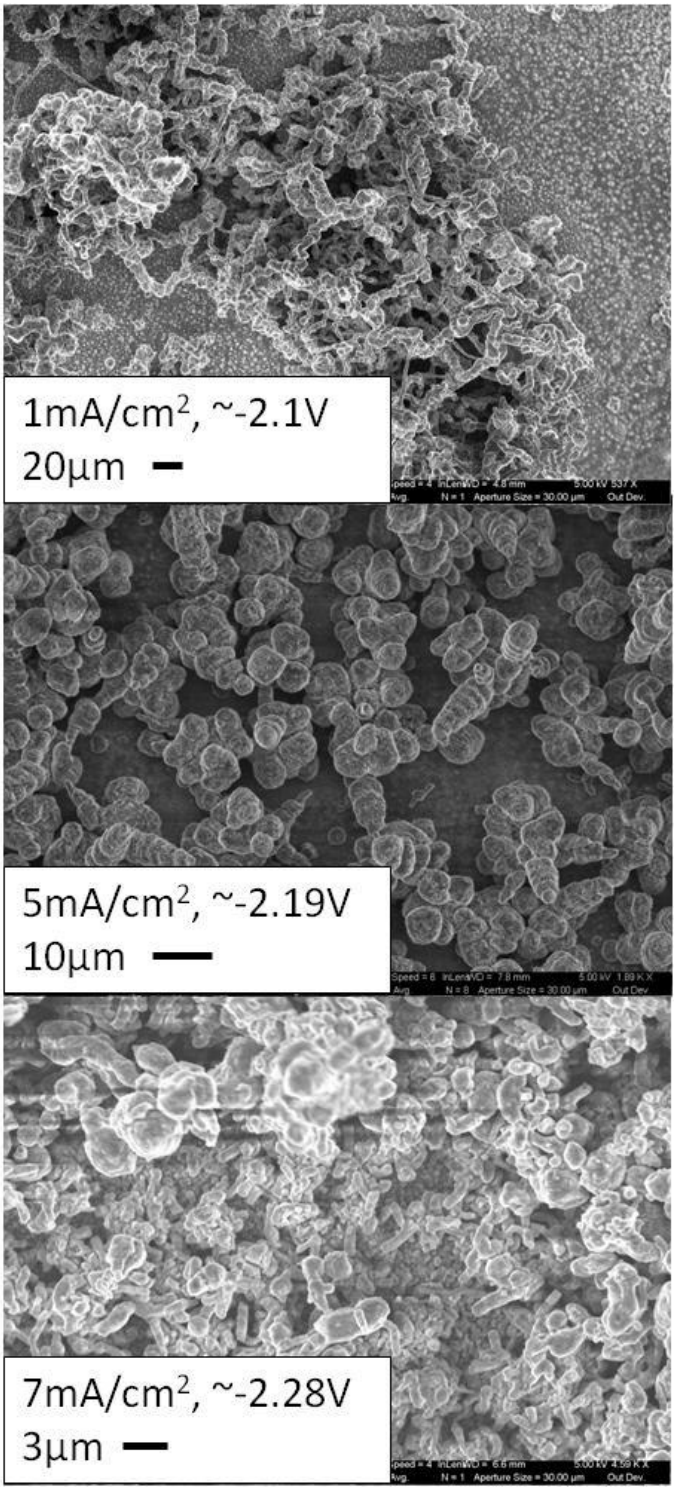

Figure 3

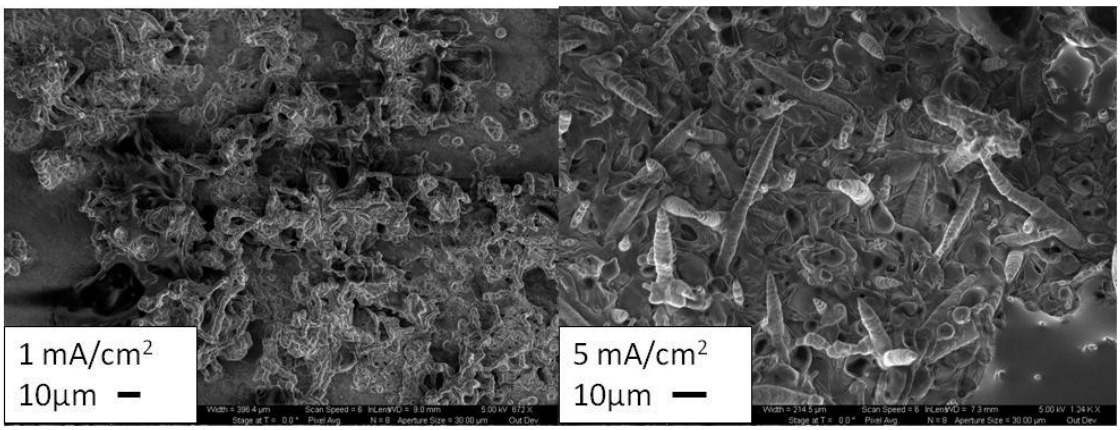

Figure 4

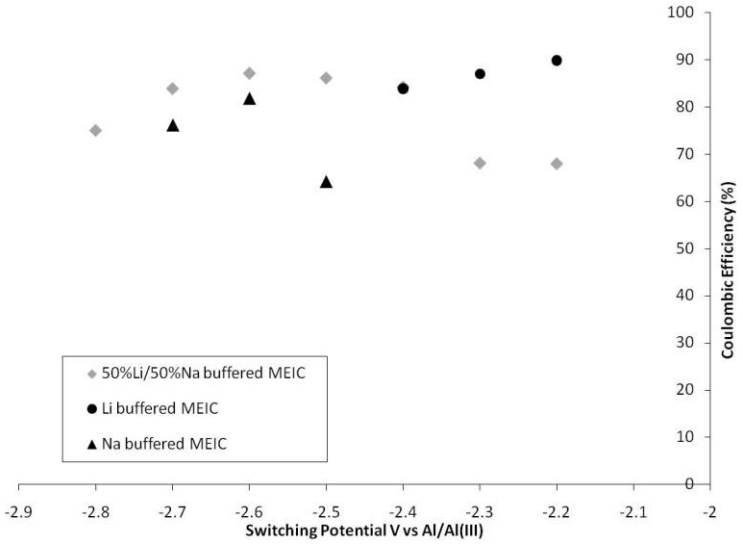
100
90
80
70
60
50
40
30
20
10
0
Coulombic Efficiency (%)
50%Li/50%Na buffered MEIC
Li buffered MEIC
Na buffered MEIC
-2.9
-2.8
-2.7
-2.6
-2.5
-2.4
-2.3
-2.2
-2.1
-2
Switching Potential V vs Al/Al(III)

Figure 5

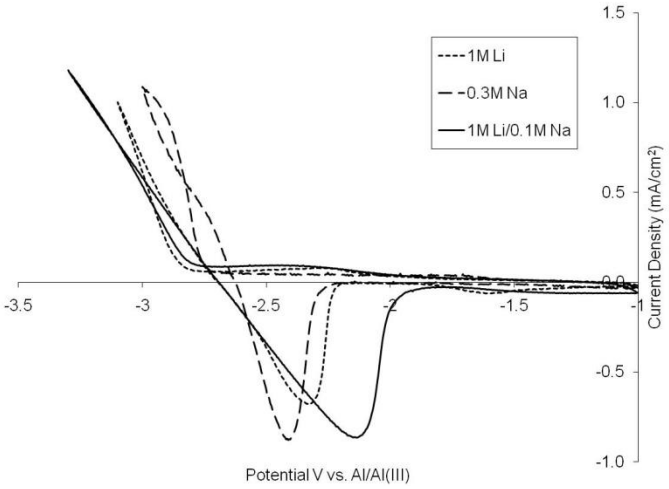
1M Li
0.3M Na
1M Li/0.1M Na
1.5
1.0
0.5
0.0
-0.5
-1.0
-3.5
-3
-2.5
-2
-1.5
-1
Current Density (mA/cm²)
Potential V vs. Al/Al(III)

Figure 6

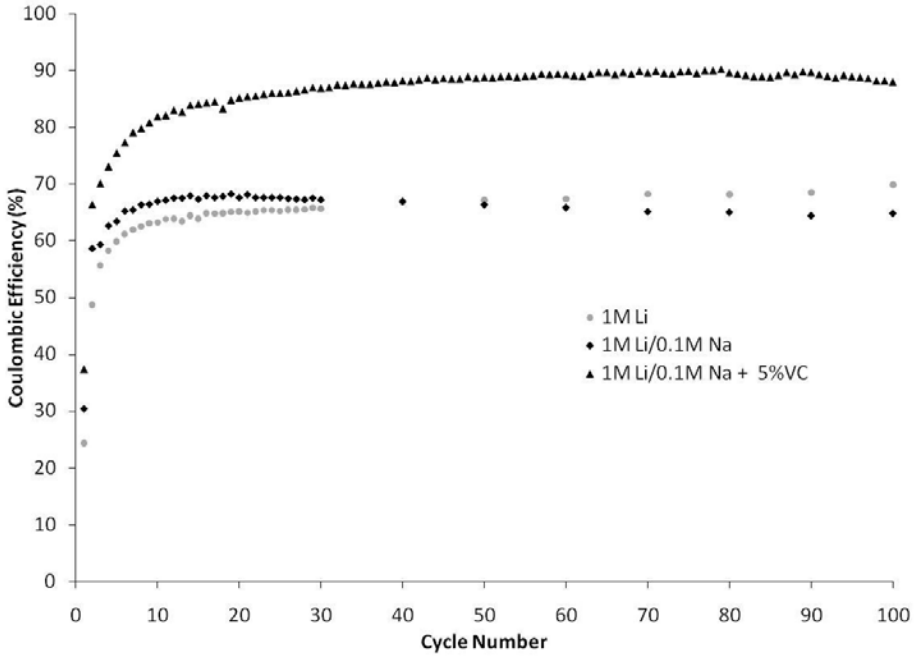
Coulombic Efficiency (%)
Cycle Number
1M Li
1M Li/0.1M Na
1M Li/0.1M Na + 5%VC
0
10
20
30
40
50
60
70
80
90
100

Figure 7

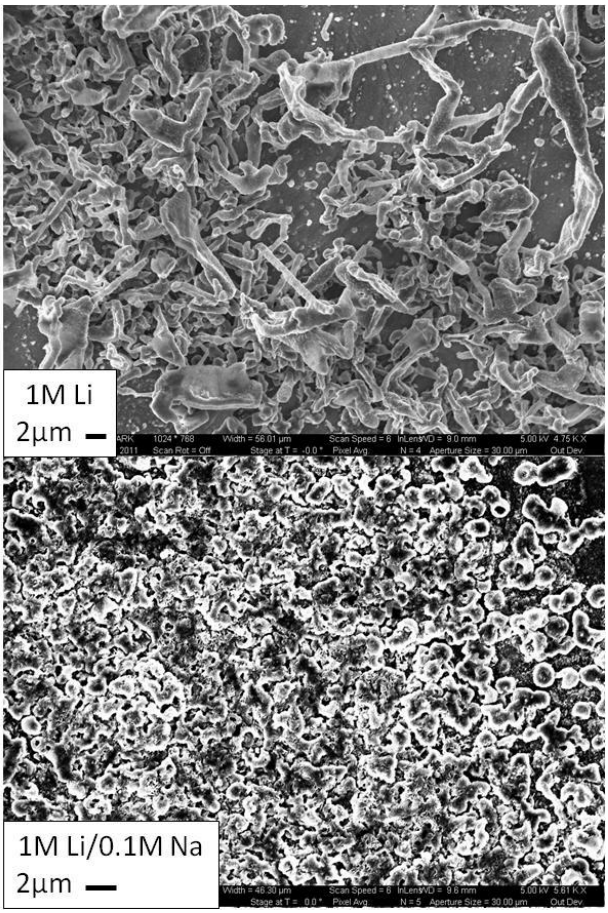

Figure 8

Disclaimer: Reference herein to any specific commercial company, product, process, or service by trade name, trademark, manufacturer, or otherwise, does not necessarily constitute or imply its endorsement, recommendation, or favoring by the United States Government or the Department of the Army (DoA). The opinions of the authors expressed herein do not necessarily state or reflect those of the United States Government or the DoA, and shall not be used for advertising or product endorsement purposes.